

OUTCOME OF SIX CANDIDATE TRANSITING PLANETS FROM A TR_{ES} FIELD IN ANDROMEDA

FRANCIS T. O'DONOVAN¹, DAVID CHARBONNEAU^{2,3}, ROI ALONSO⁴, TIMOTHY M. BROWN⁵, GEORGI MANDUSHEV⁶,
EDWARD W. DUNHAM⁹, DAVID W. LATHAM², ROBERT P. STEFANIK², GUILLERMO TORRES², MARK E. EVERETT⁷

Submitted to the Astrophysical Journal, 22 July 2006

ABSTRACT

Driven by the incomplete understanding of the formation of gas giant extrasolar planets and of their mass–radius relationship, several ground–based, wide–field photometric campaigns are searching the skies for new transiting extrasolar gas giants. As part of the Trans–atlantic Exoplanet Survey (TrES), we monitored approximately 30,000 stars ($9.5 \leq V \leq 15.5$) in a $5.7^\circ \times 5.7^\circ$ field in Andromeda with three telescopes over five months. We identified six candidate transiting planets from the stellar light curves. From subsequent follow–up observations, we rejected each of these as an astrophysical false positive, i.e. a stellar system containing an eclipsing binary, whose light curve mimics that of a Jupiter–sized planet transiting a sun–like star. We present these candidates as an example of the procedures followed by the TrES team to reject false positives from our list of candidate transiting hot Jupiters.

Subject headings: stars: planetary systems — techniques: photometric — techniques: radial velocities

1. INTRODUCTION

There are currently ten extrasolar planets for which we have measurements of both the planetary radius and mass (see Charbonneau et al. 2006a, for a review, and McCullough et al. 2006). These gas giants have been observed to transit their parents stars, and seven were first identified from such transit observations. The other three were discovered from solar neighborhood Doppler surveys that can detect the stellar reflex motion due to an orbiting massive planet, and the transits by the three planets were observed post–discovery.

The transiting planets have supplied new opportunities to study Jupiter–sized exoplanets. These “hot Jupiters” orbit within 0.05 A.U. of their star, and the incident flux on a hot Jupiter from the nearby star results in an inflated planetary radius. Current theoretical models which include this stellar insolation can account for the radii of nine of the transiting planets. However, HD 209458 b (Charbonneau et al. 2000; Henry et al. 2000) has a radius ~ 20 –30% larger than predicted (see Laughlin et al. 2005 for a review of the current structural models for insolated hot Jupiters). The mass–radius relation of known transiting gas giants less massive than Jupiter provides a test of the current planetary formation models. The “hot Saturn” HD 149026 b has a mass and radius that require a large core of approximately $70 M_{\oplus}$ (Sato et al. 2005; Charbonneau et al. 2006b), which is thought to imply

formation via core accretion (Pollack 1984; Pollack et al. 1996), rather than through gravitational instability (Boss 1997).

The anomalous radius of HD 209458 b and the sparse sampling of the mass–radius parameter space for extrasolar planets has motivated the search for new transiting planets. There are several small aperture wide–field surveys targeting these objects, such as BEST (Rauer et al. 2004), the HAT network (Bakos et al. 2002, 2004), KELT (Pepper et al. 2004), SuperWASP (Street et al. 2003), Vulcan (Borucki et al. 2001), and XO (McCullough et al. 2005), as well as deeper surveys like the Optical Gravitational Lensing Experiment (OGLE; Udalski et al. 2002) that is probing the Galactic disk. We are conducting a transit campaign, the Trans–atlantic Exoplanet Survey⁸ (TrES), using a network of three 10 cm telescopes with a wide longitudinal coverage: Sleuth (located at Palomar Observatory, California; O'Donovan et al. 2004), PSST (Lowell Observatory, Arizona; Dunham et al. 2004), and STARE⁹ (on the isle of Tenerife, Spain; Alonso et al. 2004b). The telescopes monitor over several months a $5.7^\circ \times 5.7^\circ$ field of view containing thousands of nearby bright stars ($9.5 \leq V \leq 15.5$), and we examine the light curves of stars with $V \leq 14.0$ for repeating eclipses with the short–period, small–amplitude signature of a transiting hot Jupiter. We announced our first discovery as TrES–1 (Alonso et al. 2004a), the closest planet identified using the transit method. Our target stars are bright relative to those monitored by OGLE, such as OGLE–TR–10 ($V = 15.8$; Konacki et al. 2005). Detailed atmospheric studies of these bright stars are within the capabilities of current space–based observatories (Charbonneau et al. 2002; Vidal–Madjar et al. 2003) and some ground–based observatories (Deming et al. 2005a). The proximity of TrES–1 and HD 209458 b also facilitated the first direct detections of emitted planetary radiation (Charbonneau et al. 2005; Deming et al. 2005b).

¹ California Institute of Technology, 1200 East California Boulevard, Pasadena, CA 91125; ftod@caltech.edu

² Harvard–Smithsonian Center for Astrophysics, 60 Garden Street, Cambridge, MA 02138

³ Alfred P. Sloan Research Fellow

⁴ Laboratoire d'Astrophysique de Marseille, Traverse du Siphon, 13376 Marseille 12, France

⁵ Las Cumbres Observatory Global Telescope, 6720 Cortona Drive, Suite 102, Goleta, CA 93117

⁶ Lowell Observatory, 1400 West Mars Hill Road, Flagstaff, AZ 86001

⁷ Planetary Science Institute, 1700 East Fort Lowell Road, Suite 106, Tucson, AZ 85719

⁸ [http://www.astro.caltech.edu/~sim\\$ftod/tres/](http://www.astro.caltech.edu/~sim$ftod/tres/)

⁹ <http://www.hao.ucar.edu/public/research/stare/stare.html>

For a typical TrES field at a Galactic latitude of $b \sim 15^\circ$, we find 10–20 candidates with light curves similar to that of a sun-like star transited by a Jupiter-sized planet (see, e.g., Dunham et al. 2004). We expect few of these to be true transiting planets, as there are several types of astrophysical systems whose light curves can be mistaken for that of a transiting planet. For example, a hot Jupiter and a late M dwarf are similar in size, and both produce an eclipse depth of roughly 1% across a solar type star. Another example is the eclipse of a giant star by a dwarf star, where the eclipse can have a depth of 1%. However, for a given orbital period, the eclipse duration for such a binary is much longer than the transit duration of a planet, since this duration depends on the size of the eclipsed star. Also, these systems cannot have the very short, 1 day orbital period of some of the known hot Jupiters: for a binary consisting of a solar-type star and a $10 R_\odot$ K giant, the orbital separation must exceed at least $11 R_\odot$, and correspondingly the orbital period must be greater than 4.3 days.

Brown (2003) details the most likely impostors and estimates their relative frequency. For a STARE field in Cygnus, he predicts that from every 25,000 stars observed with sufficient photometric precision to detect a transit, one can expect to identify one star with a transiting planetary companion. However, for this field near the Galactic plane ($b \sim 3^\circ$), the number of impostor systems identified as candidate planets will outnumber the true detections by an order of magnitude. (The yield of eclipsing systems from such transit surveys depends on the eclipse visibility, which is the fraction of such systems with a given orbital period for which a sufficient number of eclipses could be observed for the system to be detected. This visibility varies with weather conditions and the longitudinal coverage of the telescopes used.) Of the false positives, approximately half are predicted to be eclipsing binaries whose eclipse depths are about 1% (for example, an F+M binary with central transits or a grazing incidence F+F binary), and half to be blends, where a faint eclipsing binary and a bright star coincide on the sky or are physically associated, mixing their light and reducing the observed eclipse depth to that of a transiting planet. For each TrES target field, we follow a procedure of careful examination of each candidate, with follow-up photometry and spectroscopy to eliminate the majority of false positive detections before committing to the final series of observations with 10-m class telescopes to determine the radial velocity orbit of the candidate planet. Here we discuss our follow-up strategy (§2) and present the step-by-step results of this procedure for one of our fields in Andromeda. We describe the TrES network observations in §3, and outline the initial identification of six candidates from the stellar light curves in §4. Based on our follow-up observations of these candidates (§5), we were able to conclude that each was an astrophysical false positive (§6).

2. FOLLOW-UP OBSERVATIONS OF PLANETARY CANDIDATES

On the road to discovering a new transiting planet, we must be able to reject impostors that would lead us down a false path. The initial scientific pay-off from each new transiting hot Jupiter comes when an accurate planetary mass and radius have been determined, which can then

be used to confront models of planetary structure and formation. These determinations require a high-quality light curve together with a spectroscopic orbit for the host star.

The light curves from small wide-angle telescopes are not of sufficient quality to derive an accurate radius ratio for the purpose of both false positive rejection and planetary modeling, so high-quality follow-up photometric observations with a larger telescope are needed. Recent experience suggests that a photometric accuracy better than 1 mmag with a time resolution better than 1 minute can be achieved with a meter-class telescope at a good site, and such observations can deliver radius values good to a few percent and transit times good to 0.2 min (Holman et al. 2005, 2006). For smaller telescopes, scintillation can limit the photometric precision at this cadence (Young 1967; Dravins et al. 1998).

A practical problem for this follow-up photometry is that the transiting-planet candidates do not emerge from the wide-angle surveys until late in the observing season, when the observability of the candidates do not permit full coverage of a transit event. With only partial coverage of an event it is difficult to remove systematic drifts across the event, reducing the accuracy of the derived transit depth. Furthermore, full coverage of a transit is important for deriving very accurate transit timings. Without accurate ephemerides, the error in the predicted transit times during the next observing season may be too large to facilitate follow-up photometric observations. The typical duty cycle for a transit is a few hours over a period of a few days, i.e. a few percent. Therefore, if the follow-up photometry does not confirm a transit, the interpretation is ambiguous. The ephemeris may have been too inaccurate, or perhaps the original transit event was a photometric false detection (that is the event was caused by instrumental error, rather than a true reduction in flux from the candidate).

One approach to recovering transits and providing an updated ephemeris for high-quality photometric observations with a larger telescope is to monitor candidates with intermediate sized telescopes, such as TopHAT in the case of the HAT survey (Bakos et al. 2004), Sherlock (Kotredes et al. 2004) in the case of TrES, or teams of amateur telescopes (McCullough et al. 2006) in the case of XO.

A second approach to confirming that a candidate is actually a planet is to obtain very precise radial velocities to see whether the host star undergoes a small reflex motion as expected for a planetary companion. This approach has the advantage that the velocity of the host star varies continuously throughout the orbit, so the observations can be made at any time with only modest attention to the phasing compared to the photometric period. The ephemeris can then be updated using the velocities, to provide reliable transit predictions for the follow-up photometry. A second advantage is that a spectroscopic orbit is needed anyway to derive the mass of any candidate that proves to be a planet. The big disadvantage of this approach is that a velocity precision on the order of 10 m s^{-1} is needed, and this requires access to a large telescope with an appropriate spectrograph.

For the followup of transiting-planet candidates identified by TrES, we have adopted a strategy designed to eliminate the vast majority of astrophysical false pos-

itives with an initial spectroscopic reconnaissance using the Harvard–Smithsonian Center for Astrophysics (CfA) Digital Speedometers (Latham 1992) on the 1.5–m Wyeth Reflector at the Oak Ridge Observatory in Harvard, Massachusetts and on the 1.5–m Tillinghast Reflector at the F. L. Whipple Observatory (FLWO) on Mount Hopkins, Arizona. We aim to spectroscopically observe candidates during the same season as the discovery photometry. These instruments provide radial velocities good to better than 1 km s^{-1} for stars later than spectral type A that are not rotating too rapidly, and thus can detect motion due to stellar companions with just two or three exposures (see, e.g., Latham 2003; Charbonneau et al. 2004). Thus even if the followup is not performed until the target field is almost setting, we can still reject some candidates spectroscopically, even when photometric followup is not useful. For periods of a few days the limiting value for the mass detectable with these instruments is about 5 to 10 Jupiter masses.

The spectra obtained with these instruments also allow us to characterize the host star. We use a library of synthetic spectra to derive values for the effective temperature and surface gravity, (assuming solar metallicity), and also the line broadening. In our experience, rotational broadening of more than 10 km/s is a strong hint that the companion is a star, with enough tidal torque to synchronize the rotation of the host star with the orbital motion. Although the gravity determination is relatively crude, with an uncertainty of perhaps 0.5 in $\log g$, it is still very useful for identifying those host stars that are clearly giants with $\log g \leq 3.0$. We presume that these stars must be the third member of a system that includes a main-sequence eclipsing binary, either a physical triple or a chance alignment, and we make no further follow-up observations. Our spectroscopic classification of the host star is a first step towards the detailed spectroscopic analysis that is needed to estimate the radius and mass of the host star, so that the actual mass and the radius of the planet can be derived from the ratio of those values that come from a spectroscopic orbit and a high-quality light curve.

The combination of both spectroscopy and photometry is needed in the case of “blends”. The wide-angle surveys by necessity have broad images, typically with FWHM values of $20''$. Thus there is a significant probability of a chance alignment between a relatively bright star and a fainter eclipsing binary that just happens to be nearby on the sky. Photometric observations with high spatial resolution on a larger telescope can be used to sort out such cases by resolving the eclipsing binary (see, e.g., Charbonneau et al. 2004). In some cases these systems can also be detected using the wide-angle discovery data, by showing that there is differential image motion during the transit events, even though the eclipsing binary is unresolved. Such a candidate might pass our spectroscopic test as a solitary star with constant radial velocity.

Even after a spectroscopic orbit implying a planetary companion has been derived, care must be taken to show that the velocity shifts are not due to blending with the lines of an eclipsing binary in a triple system (e.g., Mandushev et al. 2005). It may be hard to see the lines of the eclipsing binary, partly because the eclipsing binary can be quite a bit fainter than the bright third star,

and partly because its lines are likely to be much broader due to synchronized rotation. In some cases it may be possible to extract the velocity of one or both the stars in the eclipsing binary using a technique such as TODCOR (Mandushev et al. 2005). Combining modeling of the photometric light curve and information from the spectroscopic pseudo orbit for the system can help guide the search for the eclipsing binary lines. Even if the lines of the eclipsing binary can not be resolved, a bisector analysis of the lines of the third star may reveal subtle shifts that indicate a binary companion.

If the eclipsing binary of a triple is faint enough relative to the primary star, the primary may display no radial velocity variability. However, if the color of the eclipsing binary is different enough from that of the third star, high-quality multi-color light curves will reveal the color-dependent eclipse depths indicative of a triple (see, e.g. O’Donovan et al. 2006).

Follow-up observations with 1–m class telescopes both remove astrophysical false positives from consideration and prepare for the eventual modeling of newly discovered transiting planets. In the case of our field in Andromeda, our followup ruled out all of our planet candidates, which provided us with a variety of false positives to study.

3. INITIAL OBSERVATIONS WITH THE TRES NETWORK

In August 2003, we selected a new field centered on the guide star HD 6811 ($\alpha = 01^{\text{h}}09^{\text{m}}30^{\text{s}}.13$, $\delta = +47^{\circ}14'30''.5$ J2000). We designated this target field as And0, the first TrES field in Andromeda. We observed this field with each of the TrES telescopes. Although the TrES network usually observes concurrently, in this case weather disrupted our observations. Sleuth monitored the field through an SDSS r filter for 42 clear nights between UT 2003 August 27 and October 24. STARE began its observations with a Johnson R filter on UT 2003 September 17, and observed And0 until UT 2004 Jan 13 during 23 photometric nights. PSST went to this field on UT 2003 November 14 and collected Johnson R observations until 2004 January 11, obtaining 19 clear nights. We estimate our recovery rate for transit events should be 100% for orbital periods $P < 6$ days, declining to 70% for $P = 10$ days (see Fig. 2), where our recovery criterion is the observation of at least half the transit from three distinct transit events. We used an integration time of 90 s for our exposures. During dark time, we took multicolor photometry (SDSS g , i , and z for Sleuth and Johnson B and V for PSST and STARE) for stellar color estimates.

4. SEARCHING FOR TRANSIT CANDIDATES

After each night of observation, the data were automatically transferred from the telescope computers and calibrated on our local computers. We have customized IDL routines to perform the bias-subtraction and flat-fielding of the Sleuth and STARE data. An additional dark current subtraction and shutter correction is performed for the STARE data. We apply the standard `zerocombine`, `ccdproc`, and `flatcombine` tasks in the IRAF¹⁰ package (Tody 1993) for the PSST data. We

¹⁰ IRAF is distributed by the National Optical Astronomy Observatories, which are operated by the Association of Universities for Research in Astronomy, Inc., under cooperative agreement with the National Science Foundation.

applied differential image analysis (DIA) to each of the separate photometric data sets from the three telescopes, using the following pipeline (described in Dunham et al. 2004 and O’Donovan et al. 2006, and based in part upon Alard 2000).

We first performed a spatial interpolation on our science images so that the pixel coordinates of a given star were the same in each image. We selected 10 images recorded at low air mass on a photometric night during dark time, and averaged these to produce a reference image. We applied profile-fitting (PSF) photometry (DAOPHOT II/ALLSTAR; Stetson 1987, 1992) to the reference image to produce a standard list of stars and image coordinates. We computed the corresponding coordinates (α, δ) for the standard stars by cross-referencing a subset with the Tycho-2 Catalog (Høg et al. 2000b). For each science image, we generated a list of stars using code similar to Stetson’s FIND and identified the stars present in both this list and the standard star list using Stetson’s DAOMASTER routine. We cross-correlated the reference image with the science image to compute the approximate (x, y) offset, with an accuracy of 1–2 pixels. (Most of the offsets were between one and five pixels.) Using the list of matched stars and this rough offset, we derived the (x, y) quadratic transformations to match the image star coordinates with those from this standard list and spatially interpolated the science image.

Next, we obtained the differential magnitudes of the stars in our interpolated images with reference to a master image. We produced this master image by combining 20, 18, and 15 of the best-quality interpolated images in our Sleuth, PSST and STARE data sets, respectively. We subtracted our interpolated images from this master image, using a second-order polynomial in x and y as our convolution kernel over the entire frame. Assuming the centroids from the standard star list, we computed the differential magnitude relative to the ensemble average of each standard star in each subtracted image using aperture photometry and generated time series of these relative magnitudes. Since small-aperture, wide-field surveys such as TrES often suffer from systematics (caused, for example, by variable atmospheric extinction), we decorrelated these time series as follows. We grouped our standard stars, ordered by increasing magnitude, into batches of 500. For each light curve in a given batch, we computed the linear combination of the other light curves in that batch that was the least-squares fit to the selected light curve, and subtracted this fit from the light curve.

Initially, we examined our Sleuth observations separately, as these dominate the TrES data set, providing 50% of the data. Our Sleuth data consisted of 10143 observations with a cadence of 115 s. Before performing our computationally intensive transit search, we averaged each time series in 9 minute wide bins, reducing the number of time steps to 2357, while keeping sufficient temporal resolution to resolve the duration of a central transit (about 3 hours). The rms scatter of the binned data was below 0.015 mag for approximately 7,800 stars. If we observed three distinct transits of one of these stars with at least half coverage per event, as required for detection, we would obtain 30 binned data points during transit (assuming a transit duration of 3 hours), each with a pre-

cision of better than 1.5%. The detection of a 1% transit would therefore have a confidence level of at least 4σ . We searched the time series for periodic transit-like dips using the box-fitting least squares transit-search algorithm (BLS; Kovács, Zucker, & Mazeh 2002), which assigns a Signal Detection Efficiency (SDE) statistic to each star, based on the strength of the transit detection. We restricted our search to periods ranging from 0.1 to 10 days. Having sorted the stars in order of decreasing magnitude and decreasing SDE, we visually examined each stellar light curve (phased to the best fit period derived by the algorithm) in turn, until we determined that we could no longer distinguish a transit signal from the noise. We identified six transit candidates (see Tables 1 and 2, and Fig. 1).

We then combined the three TrES data sets, which optimized our visibility function (see Fig. 2), and allowed us to confirm the detection of real eclipse events from simultaneous observations from multiple telescopes. We produced the combined TrES data set as follows. For each star in the Sleuth standard star list, we attempted to identify the corresponding stars in the other two lists. We computed the distances between a given Sleuth standard star and the PSST standard stars, and matched the Sleuth star with a PSST star if their angular separation was less than $5''$ (0.5 pixels). Because of the slight differences in the chosen filter and field of view, some Sleuth stars did not have corresponding PSST stars. We created a new standard star list from the Sleuth and PSST star lists, with only one entry for each pair of matched stars and an entry for each unmatched star. We then repeated this procedure with this new star list and the STARE list to produce the TrES field standard star list. For each star, we then combined the relevant time series, and chronologically reordered the data. Our combined data set consisted of 20505 observations, or 4666 time steps after binning. The rms scatter of the averaged TrES data was below 0.015 mag for 9,148 stars (see Fig. 3) out of the 29,259 stars in the field. We repeated the BLS transit-search, but did not identify any new candidates (see Fig. 4). From Figure 2, we can see that a visibility of 80% had already been achieved for $P < 5$ d for the Sleuth data alone, hence the addition of the STARE and PSST data did not significantly increase the detection space. Hence the lack of additional candidates is not surprising. We proceeded to our follow-up observations of these six candidates with larger telescopes.

5. FOLLOWUP OF AND0 CANDIDATES

Many of the bright stars within our field were also observed as part of other surveys. We identified our candidates in online catalogs and compared these observations with our expectations based on the planet hypothesis. We found Tycho-2 (Høg et al. 2000a,b) visible ($B_T - V_T$) colors for two of our candidates, and Two Micron All Sky Survey (2MASS; Cutri et al. 2003) infrared ($J - K$) colors for all six (see Tab. 3). We searched the USNO CCD Astrograph Catalog (UCAC2; Zacharias et al. 2004) for the proper motions of the stars. All of the candidates display a measurable proper motion, consistent with nearby dwarfs. However, these proper motions were not sufficiently large to rule out distant, high-velocity giants.

Finally, we retrieved Digitized Sky Survey¹¹ (DSS) images of the sky surrounding each candidate to check for possible nearby stars of similar brightness within our PSF radius. None were found.

We observed the six And0 candidates starting on UT 2004 September 28 using the Harvard–Smithsonian Center for Astrophysics (CfA) Digital Speedometers (Latham 1992). These spectrographs cover 45Å centered on 5187Å and have a resolution of 8.5 km s⁻¹ (a resolving power of $\lambda/\Delta\lambda \approx 35,000$). We cross-correlated our spectra against a grid of templates from our library of synthetic spectra to estimate various stellar parameters of our targets and their radial velocities. J. Morse computed this spectral library, using the Kurucz model atmospheres (J. Morse & R. L. Kurucz, 2004, private communication). Assuming a solar metallicity, we estimated the effective temperature (T_{eff}), surface gravity (g) and rotational velocity ($v \sin i$) for each candidate (see Tab. 3) from the template parameters that gave the highest average peak correlation value over all the observed spectra.

For the three candidates with low stellar rotation, $v \sin i < 50 \text{ km s}^{-1}$, we obtained several spectra over different observing seasons to determine the radial velocity variation of each star. Table 4 details our spectroscopic observations. For these slowly rotating candidates, the typical precision for our spectroscopic parameters is $\Delta T_{\text{eff}} = 150 \text{ K}$, $\Delta \log g = 0.5$, $\Delta v \sin i = 2 \text{ km s}^{-1}$ and $\Delta V = 0.5 \text{ km s}^{-1}$. The precision of the estimates degrades for stars with large $v \sin i$ values or few spectroscopic observations.

We obtained high precision photometry of T–And0–03874 on UT 2004 December 19 using the Minicam CCD imager at the FLWO 1.2-m telescope on Mt. Hopkins, Arizona. Minicam consists of two 2248×4640 pixel thinned, backside–illuminated Marconi CCDs mounted side–by–side to span a field of approximately 20.4×23.1 arcminutes bisected by a narrow gap. We employed 2×2 pixel binning for an effective plate scale of 0.6'' pixel⁻¹ and read out each half CCD through a separate amplifier. We offset the telescope to place T–And0–03874 centrally on one amplifier region and autoguided on the field. We obtained concurrent light curves in 3 filters by cycling continuously through the SDSS g , r , and z filters with exposure times of 90, 45, and 90 seconds respectively. The seeing was poor (FWHM ~ 3 –7'') and varied throughout our observations. Unfortunately, high winds forced us to close the dome during the night and we obtained only partial coverage of the predicted event. Late in the scheduled observations, we re–opened for a short time.

We subtracted the overscan bias level from each image and divided each by a normalized flat field constructed from the filtered mean of twilight sky exposures. To construct a light curve of T–And0–03874 and neighboring bright stars, we located the stars in each image. We measured stellar fluxes in a circular aperture and subtracted the sky as estimated by the median flux in an

annulus centered on the star (iteratively rejecting deviant sky pixel values). We used a relatively large 12'' radius aperture and sky annulus with inner and outer radii of 15'' and 27'' respectively in an effort to reduce systematic errors arising due to the poor and variable seeing conditions. We first corrected the flux of each star by an amount proportional to its airmass in each exposure by using extinction coefficients for each filter based on previous experience with Minicam photometry. Second, we selected a group of bright, uncrowded stars near T–And0–03874 as potential comparison stars. In each exposure, we calculated the mean flux of the comparison stars weighted according to brightness. We assumed that any variations in this mean flux represented extinction in each image and used them to apply corrections to each light curve. We then inspected by eye the light curve of each comparison star, and fit the light curves to models of constant brightness to find chi-squared statistics. We removed from our group of comparison stars any star that showed significant variations. We recalculated the extinction corrections iteratively in this manner until we achieved no variation in the comparison star light curves. We accepted 29, 32, and 4 comparison stars for the g , r , and z band light curves respectively. Finally, we normalized the flux in the light curves of T–And0–03874 with respect to the out–of–eclipse data.

6. REJECTING FALSE POSITIVE DETECTIONS

Based on our detailed investigations of the candidates, we eliminated each And0 candidate as follows.

In the case of T–And0–00948, both the Sleuth (Fig. 1) and the TrES (Fig. 4) light curves show a secondary eclipse. The low surface gravity ($\log g = 3.0$) is that of a distant giant star, consistent with the red color $J-K = 0.60$ (since the majority of stars with $J-K > 0.5$ are expected to be giants see, e.g. Brown 2003). There was no observed variation in the radial velocity of this candidate ($v_r = -28.82 \text{ km s}^{-1}$). T–And0–00948 is most likely the primary star of a diluted triple system.

Upon further examination of the individual light curves for T–And0–01241, we noticed that only Sleuth had observed transit events for this system. Neither PSST nor STARE had observed this field during the time of the Sleuth transit events, preventing a comparison of the light curves. Based on the Sleuth data, we predicted the times of transits during the entire TrES And0 campaign. STARE did observe T–And0–01241 at a time at which it was predicted to transit but did not observe the transit. It was therefore possible that this was a photometric false positive. We then obtained sufficient evidence from the follow–up spectroscopy to discount this system. A dwarf with $\log g = 4.5$, the star has the high effective temperature ($T_{\text{eff}} = 9500 \text{ K}$) and blue colors ($J - K = 0.01$) of an early A star. Figure 5b shows the nearly featureless spectrum of this star. For such a large star with a radius $R \sim 2.7 R_{\odot}$, the observed transit depth of 0.9% indicates a non-planetary size ($R = 2.5 R_{\text{Jup}}$) for the eclipsing body.

The radial velocity of T–And0–02022 varies with an amplitude corresponding to a stellar–mass companion. We determined this system to be an eclipsing binary, comprised of a slightly evolved F dwarf and an M dwarf. This system has a mass function $f(M) = 0.0304 \pm 0.0013 M_{\odot}$ and an eccentricity of 0.027 ± 0.014 . As

¹¹ The Digitized Sky Survey (<http://archive.stsci.edu/dss/>) was produced at the Space Telescope Science Institute under U.S. Government grant NAG W-2166. The images of these surveys are based on photographic data obtained using the Oschin Schmidt Telescope on Palomar Mountain and the UK Schmidt Telescope. The plates were processed into the present compressed digital form with the permission of these institutions.

suming an orbital inclination of $i \sim 90^\circ$, and a mass of $1.6 M_\odot$ consistent with the effective temperature ($T_{\text{eff}} = 7000 \text{ K}$), we estimated the mass of the companion to be $m = 0.5 M_\odot$. Figure 6 shows the radial velocity orbit. The circular orbit of T-And0-02022 allows us to constrain the stellar radius, independent of our derived spectral type and luminosity class. The circular orbit implies orbital synchronization and orbital-rotation axes alignment, since circularization has the longest timescale of these processes (see Hut 1981 for a derivation of these timescales for close binary systems and a comparison for different binary mass ratios and moments of inertia of the primary star). We can therefore assume that the stellar rotation period is the same as the orbital period of 4.7399d. We then use the observed rotational broadening ($v \sin i = 22 \text{ km s}^{-1}$) to estimate the radius of the star to be $2.0 R_\odot$. Future photometric observations of this systems with KeplerCam (Szentgyorgyi et al. 2005) are planned to more precisely measure the eclipse depth, and to derive the radius and true mass of each star in this binary (Fernandez et al., in preparation).

T-And0-02462 is a rapid rotator with $v \sin i = 77 \text{ km s}^{-1}$, and displays rotationally broadened lines (see Figure 5d), limiting the possibility of detecting the radial velocity variation caused by a planet. Regardless, a secondary eclipse is evident from the TrES light curve of T-And0-02462 (see Fig. 4), implying a binary nature for this candidate. Interestingly, the BLS best-fit period for our TrES observations of T-And0-02462 is twice that derived from the Sleuth data alone. When the Sleuth data are phased to the TrES period, the secondary eclipse is not visible, due to inadequate coverage at that phase. This resulted in a derived period half that of the true period.

The red color of T-And0-03874 ($J - K = 0.66$) and the effective temperature ($T_{\text{eff}} = 5500 \text{ K}$) calculated from the spectrum shown in Figure 5e are consistent with an early K-type star. The radial velocity of T-And0-03874 was observed to remain constant at -15.53 km s^{-1} . However, the low estimated surface gravity ($\log g = 3.5$) suggested this star is a giant star and part of diluted triple. The photometric follow-up (see Fig. 7) failed to recover transits of T-And0-03874, but did observe a nearby eclipsing binary T-And0-02943 undergoing a deep eclipse at the predicted transit time (also shown in Fig. 7). When we examined our TrES observations for T-And0-02943, we saw that the period of this eclipsing binary was that originally derived for T-And0-03874, namely 2.654 days. This eclipsing system lies $45''$ away from T-And0-03874, comparable to the PSF radius of our TrES aperture fitting ($30''$; 3 pixels). The angular resolution ($\sim 1'' \text{ pixel}^{-1}$) of the 1.2-m photometry is higher than that of the original TrES photometry ($9.9'' \text{ pixel}^{-1}$); hence the light from these two systems is blended in our TrES observations (see Fig. 8) but is

resolved in the 1.2-m photometry.

Finally, the observed parameters for T-And0-03912 ($\log g = 3.5$, $T_{\text{eff}} = 7750 \text{ K}$, $J - K = 0.25$) again imply a large stellar radius ($R \sim 1.8 R_\odot$). In order to produce the 0.9% transit, a companion radius of $1.5 R_{\text{Jup}}$ is required. This is larger than the radii of the known transiting planets, the largest of which (HD 209458b) has a radius of $1.32 \pm 0.03 R_{\text{Jup}}$ (Knutson et al. 2006). T-And0-03912 is also rapidly rotating ($v \sin i = 88 \text{ km s}^{-1}$; see Fig. 5f).

7. DISCUSSION

The Trans-atlantic Exoplanet Survey monitors $\sim 30,000$ stars each year with the photometric precision required to detect 1% transits, and from which we identify ~ 30 stars whose light curves show periodic eclipses consistent with the passage of a Jupiter-sized planet in front of a sun-like star. In order to eliminate astrophysical false positives, we have established a procedure of multi-epoch photometric and moderate-precision spectroscopic follow-up. Surviving candidates are optimal targets for high-precision multi-epoch radial velocity measurements that will yield the masses of planetary companions.

The TrES field in Andromeda was one of the first of our fields for which we combined the data from the three TrES telescopes. It has provided us with several examples of the astrophysical false positives that will be encountered in any ground-based, wide-field transit survey, all of which were rejected as a result of follow-up observations. In comparison to other, more subtle examples (such as those discussed by O'Donovan et al. 2006, Torres et al. 2004, and Mandushev et al. 2005), these were easily identified as false positives. These examples demonstrate the need for both spectroscopic and photometric follow-up of transit candidates, which may be accomplished with the 1-m-class telescopes, on which time is readily available. This ensures that the precious resource of 10-m spectroscopy is used efficiently.

FTOD and DC thank Lynne Hillenbrand for her supervision of this thesis work. This material is based upon work supported by the National Aeronautics and Space Administration under grant NNG05GJ29G, issued through the Origins of Solar Systems Program. We acknowledge support for this work from NASA's *Kepler* mission. This research has made use of the SIMBAD database, operated at CDS, Strasbourg, France, and NASA's Astrophysics Data System Bibliographic Services. This publication also utilizes data products from the Two Micron All Sky Survey, which is a joint project of the University of Massachusetts and the Infrared Processing and Analysis Center/California Institute of Technology, funded by the National Aeronautics and Space Administration and the National Science Foundation.

Facilities: PO:Sleuth, FLWO:1.2m, FLWO:1.5m

REFERENCES

- Alard, C. 2000, *A&AS*, 144, 363
 Alonso, R., et al. 2004a, *ApJ*, 613, L153
 Alonso, R., Deeg, H. J., Brown, T. M., & Belmonte, J. A. 2004b, *Astron. Nachr.*, 325, 594
 Bakos, G., Noyes, R. W., Kovács, G., Staneek, K. Z., Sasselov, D. D., & Domsa, I. 2004, *PASP*, 116, 266
 Bakos, G. Á., Lázár, J., Papp, I., Sári, P., & Green, E. M. 2002, *PASP*, 114, 974
 Borucki, W. J., Caldwell, D., Koch, D. G., Webster, L. D., Jenkins, J. M., Ninkov, Z., & Showen, R. 2001, *PASP*, 113, 439
 Boss, A. P. 1997, *Science*, 276, 1836
 Brown, T. M. 2003, *ApJ*, 593, L125
 Charbonneau, D., et al. 2005, *ApJ*, 626, 523

- Charbonneau, D., Brown, T. M., Burrows, A., & Laughlin, G. 2006a, in *Protostars and Planets V*, ed. B. Reipurth, D. Jewitt, & K. Keil (Tucson: Univ. of Arizona Press), in press, (astro-ph/0603376)
- Charbonneau, D., Brown, T. M., Dunham, E. W., Latham, D. W., Looper, D. L., & Mandushev, G. 2004, in *AIP Conf. Proc. 713: The Search for Other Worlds*, ed. S. S. Holt & D. Deming (New York: AIP), 151
- Charbonneau, D., Brown, T. M., Latham, D. W., & Mayor, M. 2000, *ApJ*, 529, L45
- Charbonneau, D., Brown, T. M., Noyes, R. W., & Gilliland, R. L. 2002, *ApJ*, 568, 377
- Charbonneau, D., et al. 2006b, *ApJ*, 636, 445
- Cutri, R. M., et al. 2003, <http://irsa.ipac.caltech.edu/applications/Gator>
- Deming, D., Brown, T. M., Charbonneau, D., Harrington, J., & Richardson, L. J. 2005a, *ApJ*, 622, 1149
- Deming, D., Seager, S., Richardson, L. J., & Harrington, J. 2005b, *Nature*, 434, 740
- Dravins, D., Lindegren, L., Mezey, E., & Young, A. T. 1998, *PASP*, 110, 610
- Dunham, E. W., Mandushev, G. I., Taylor, B. W., & Oetiker, B. 2004, *PASP*, 116, 1072
- Henry, G. W., Marcy, G. W., Butler, R. P., & Vogt, S. S. 2000, *ApJ*, 529, L41
- Høg, E., et al. 2000a, *A&A*, 357, 367
- Høg, E., et al. 2000b, *A&A*, 355, L27
- Holman, M. J., et al. 2006, *ApJ*, in press (astro-ph/0607571)
- Holman, M. J., Winn, J. N., Stanek, K. Z., Torres, G., Sasselov, D. D., Allen, R. L., & Fraser, W. 2005, *ApJ*, in press (astro-ph/0506569)
- Holt, S. S., & Deming, D., ed. 2004, *The Search for Other Worlds*
- Hut, P. 1981, *A&A*, 99, 126
- Knutson, H., Charbonneau, D., Noyes, R. W., Brown, T. M., & Gilliland, R. L. 2006, *ApJ*, submitted (astro-ph/0603542)
- Konacki, M., Torres, G., Sasselov, D. D., & Jha, S. 2005, *ApJ*, 624, 372
- Kotredes, L., Charbonneau, D., Looper, D. L., & O'Donovan, F. T. 2004, in *AIP Conf. Proc. 713: The Search for Other Worlds*, ed. S. S. Holt & D. Deming, 173
- Kovács, G., Zucker, S., & Mazeh, T. 2002, *A&A*, 391, 369
- Lasker, B. M., Sturch, C. R., McLean, B. J., Russell, J. L., Jenkner, H., & Shara, M. M. 1990, *AJ*, 99, 2019
- Latham, D. W. 1992, in *ASP Conf. Ser. 32: Complementary Approaches to Double and Multiple Star Research*, ed. H. A. McAlister & W. I. Hartkopf, IAU Colloq. 135 (San Francisco: ASP), 110
- Latham, D. W. 2003, in *ASP Conf. Ser. 294: Scientific Frontiers in Research on Extrasolar Planets*, ed. D. Deming & S. Seager (San Francisco: ASP), 409
- Laughlin, G., Wolf, A., Vanmunster, T., Bodenheimer, P., Fischer, D., Marcy, G., Butler, P., & Vogt, S. 2005, *ApJ*, 621, 1072
- Mandushev, G., et al. 2005, *ApJ*, 621, 1061
- McCullough, P. R., Stys, J. E., Valenti, J. A., Fleming, S. W., James, K. A., & Heasley, J. N. 2005, *PASP*, 117, 783
- McCullough, P. R., et al. 2006, *ApJ*, in press (astro-ph/0605414)
- O'Donovan, F. T., Charbonneau, D., & Kotredes, L. 2004, in *AIP Conf. Proc. 713: The Search for Other Worlds*, ed. S. S. Holt & D. Deming, 169
- O'Donovan, F. T., et al. 2006, *ApJ*, 644, 1237
- Pepper, J., Gould, A., & Depoy, D. L. 2004, in *AIP Conf. Proc. 713: The Search for Other Worlds*, ed. S. S. Holt & D. Deming, 185
- Pollack, J. B. 1984, *ARA&A*, 22, 389
- Pollack, J. B., Hubickyj, O., Bodenheimer, P., Lissauer, J. J., Podolak, M., & Greenzweig, Y. 1996, *Icarus*, 124, 62
- Rauer, H., Eislöffel, J., Erikson, A., Guenther, E., Hatzes, A. P., Michaelis, H., & Voss, H. 2004, *PASP*, 116, 38
- Sato, B., et al. 2005, *ApJ*, 633, 465
- Stetson, P. B. 1987, *PASP*, 99, 191
- Stetson, P. B. 1992, in *ASP Conf. Ser. 25: Astronomical Data Analysis Software and Systems I*, ed. D. M. Worrall, C. Biemesderfer, & J. Barnes, 297
- Street, R. A., et al. 2003, in *ASP Conf. Ser. 294: Scientific Frontiers in Research on Extrasolar Planets*, ed. D. Deming & S. Seager, 405
- Szentgyorgyi, A. H., et al. 2005, *American Astronomical Society Meeting Abstracts*, 207, 110.10
- Tody, D. 1993, in *ASP Conf. Ser. 52: Astronomical Data Analysis Software and Systems II*, ed. R. J. Hanisch, R. J. V. Brissenden, & J. Barnes (San Francisco: ASP), 173
- Torres, G., Konacki, M., Sasselov, D. D., & Jha, S. 2004, *ApJ*, 614, 979
- Udalski, A., et al. 2002, *Acta Astron.*, 52, 1
- Vidal-Madjar, A., Lecavelier des Etangs, A., Désert, J.-M., Ballester, G. E., Ferlet, R., Hébrard, G., & Mayor, M. 2003, *Nature*, 422, 143
- Young, A. T. 1967, *AJ*, 72, 747
- Zacharias, N., Urban, S. E., Zacharias, M. I., Wycoff, G. L., Hall, D. M., Monet, D. G., & Rafferty, T. J. 2004, *AJ*, 127, 3043

TABLE 1
 TRES LABELS FOR AND0 CANDIDATE PLANETS, TOGETHER
 WITH CORRESPONDING 2MASS AND GSC DESIGNATIONS AND
 INSTRUMENTAL V MAGNITUDE.

Candidate	2MASS ^a	GSC ^b	V
T-And0-00948	01083088+4938442	03272-00845	11.4
T-And0-01241	00531053+4717320	03266-00642	11.6
T-And0-02022	01023745+4808421	03267-01450	12.0
T-And0-02462	01180059+4927124	03272-00540	12.2
T-And0-03874	00545421+4805505	03266-00119	12.7
T-And0-03912	00595445+4902030	03271-01102	12.7

^aDesignations from 2MASS Catalog (Cutri et al. 2003), giving the coordinates of the sources in the form hhmmss.ss+ddmmss.s J2000.

^bGSC Catalog (Lasker et al. 1990).

TABLE 2
 TRANSIT PROPERTIES FOR THE SIX TRES AND0 CANDIDATES.

Candidate	SDE	Depth (mag)	Period (Days)	Duration (Hours)	N ^a	Telescope(s) ^b	True Nature
T-And0-00948	19.3	0.005	1.1198	1.6	7	S,T	Eclipsing binary
T-And0-01241	9.6 ^c	0.009	4.6619	3.4	2	S	A-type star
T-And0-02022	13.8	0.017	4.7399	3.4	5	S,P,T	Eclipsing binary
T-And0-02462	21.5	0.019	3.0691	2.2	3	S,P	Eclipsing binary
T-And0-03874	12.7	0.007	2.6540	3.2	7	S,P	Blend
T-And0-03912	18.2	0.007	2.3556	3.4	7	S,P,T	Rapidly rotating A-type star

^aThe number of distinct transits observed in the TrES data set.

^bTrES telescopes that detected transits of this candidate, where S is Sleuth, P is PSST, and T is STARE.

^cHere the SDE is based on the Sleuth data set, rather than the TrES combined observations.

TABLE 3
 PHOTOMETRIC AND SPECTROSCOPIC PROPERTIES OF THE SIX TRES AND0 CANDIDATES.

Candidate	v_r ^a (km s ⁻¹)	$P(\chi^2)$ ^b	T_{eff} ^c (K)	$\log g$ ^c	$v \sin i$ ^c (km s ⁻¹)	μ ^d (mas yr ⁻¹)	$B_T - V_T$ ^e (mag)	$J - K$ ^f (mag)
T-And0-00948	-28.82 ± 0.53	0.180	5250	3.0	3	3.0	0.87	0.60
T-And0-01241	-13.05 ± 4.06	...	9500	4.5	55	7.7	-0.07	0.01
T-And0-02022	4.47 ± 27.87	0.000	7000	3.5	22	3.5	...	0.24
T-And0-02462	-11.31 ± 4.73	0.008	6250	3.5	77	5.5	...	0.14
T-And0-03874	-15.41 ± 0.31	0.747	5500	3.5	2	6.0	...	0.66
T-And0-03912	-35.26 ± 3.43	...	7750	3.5	88	8.2	...	0.25

^aThe mean radial velocity.

^bThe probability that the observed chi-square should be less than a value χ^2 , assuming that our model of a star without radial velocity variation is correct.

^cFor a discussion of the errors in these spectroscopic data, see Section 6.

^dUCAC2 proper motions (Zacharias et al. 2004).

^eTycho-2 visible colors (Høg et al. 2000a,b).

^f2MASS infrared colors (Cutri et al. 2003).

TABLE 4
 TIME OF OBSERVATION, ORBITAL PHASE AND RADIAL VELOCITY FOR SPECTROSCOPIC
 OBSERVATIONS OF THE SIX TRÉS AND0 CANDIDATES.

Candidate	Time of Observation HJD	Photometric Orbital Phase	Radial Velocity km s^{-1}
T-And0-00948	2453276.8749	0.46	-28.16 ± 0.36
...	2453277.8530	0.33	-29.19 ± 0.40
...	2453278.8236	0.20	-29.00 ± 0.32
T-And0-01241	2453276.8062	0.73	-13.05 ± 4.06
T-And0-02022	2453276.8642	0.80	35.46 ± 0.74
...	2453301.8475	0.07	-14.14 ± 0.99
...	2453334.7734	0.02	-3.77 ± 0.94
...	2453548.9711	0.21	-39.63 ± 1.12
...	2453575.9740	0.90	24.54 ± 1.05
...	2453576.9683	0.11	-20.34 ± 1.16
...	2453626.9029	0.65	23.98 ± 1.13
...	2453627.9043	0.86	29.37 ± 0.70
...	2453628.8392	0.06	-9.31 ± 0.81
...	2453629.8518	0.27	-42.28 ± 1.12
...	2453630.8361	0.48	-15.29 ± 1.24
...	2453631.8335	0.69	30.93 ± 0.86
...	2453632.8135	0.90	24.80 ± 0.87
...	2453633.8047	0.10	-20.66 ± 1.02
...	2453636.8830	0.75	37.44 ± 0.86
...	2453779.5864	0.84	29.64 ± 1.14
T-And0-02462	2453276.8864	0.11	-7.55 ± 1.40
...	2453686.7688	0.18	-14.50 ± 3.74
T-And0-03874	2453276.8192	0.17	-15.81 ± 0.44
...	2453277.8381	0.55	-15.15 ± 0.41
...	2453301.8342	0.59	-15.09 ± 0.43
...	2453334.7619	0.00	-15.50 ± 0.43
T-And0-03912	2453276.8398	0.22	-35.26 ± 3.43

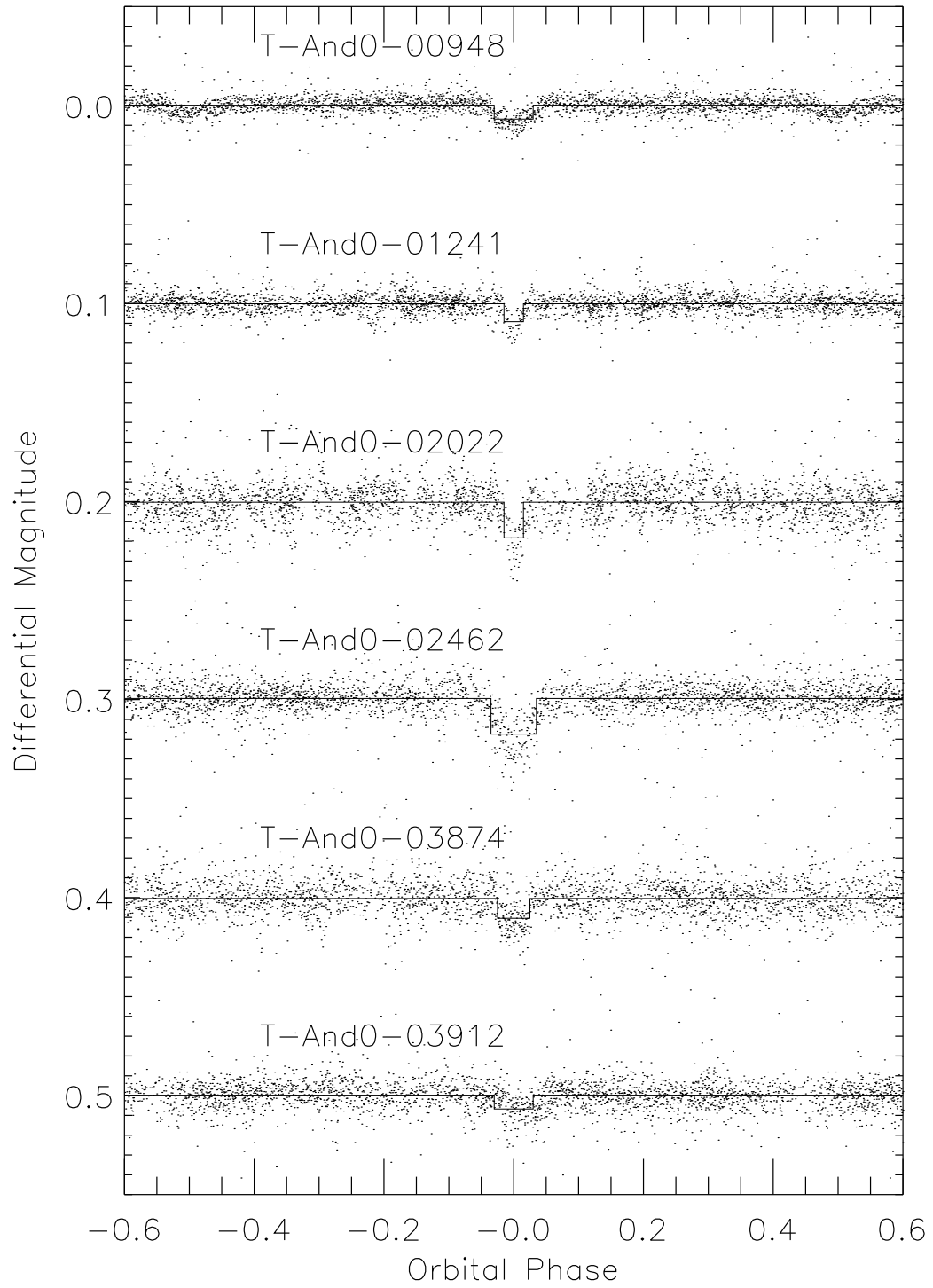


FIG. 1.— The light curves of six TrES candidates from our initial transit search of the Sleuth observations of the And0 field in Andromeda. The timeseries have been phased to the best-fit period identified by the box-fitting algorithm of Kovács et al. (2002). The corresponding box-fit light curve is overplotted.

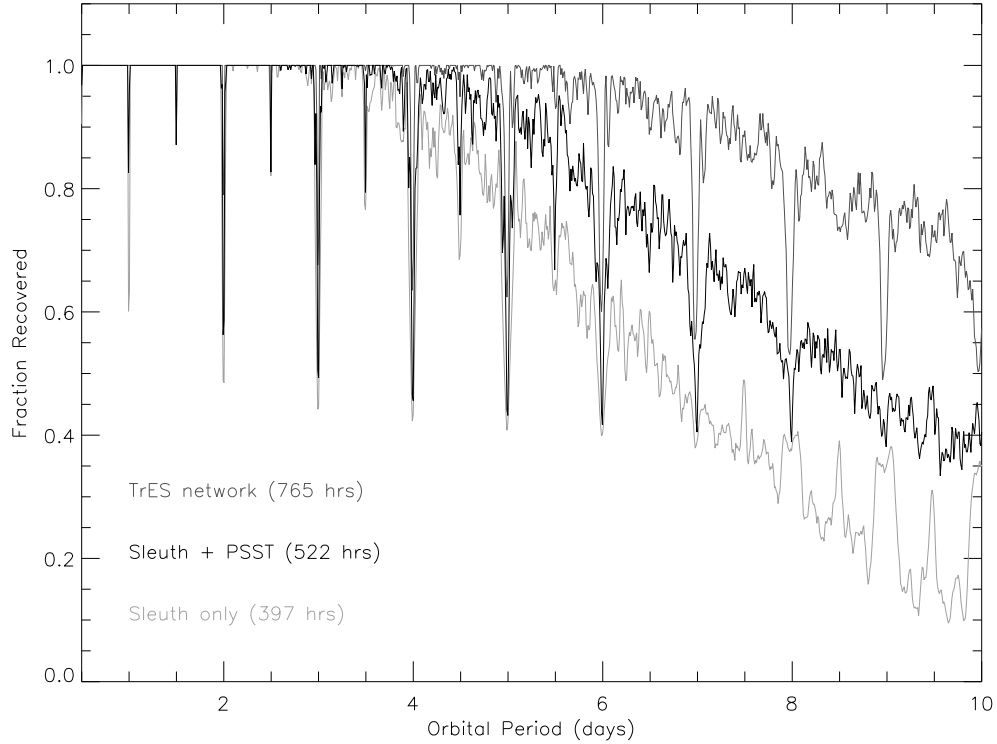


FIG. 2.— Transit visibility plot for the Andromeda field calculated from observations made using Sleuth alone (*light gray*); Sleuth and the PSST (*black*); and all three TrES telescopes (*dark gray*). The fraction of transit signals with a given period identifiable from the data is plotted, assuming a requirement of observing 3 distinct transit events, with coverage of at least half of each individual event. About 80% of transit events with periods less than 8 days should be recoverable from the TrES observations, whereas the Sleuth observations alone provide 80% coverage only up to 5 day periods.

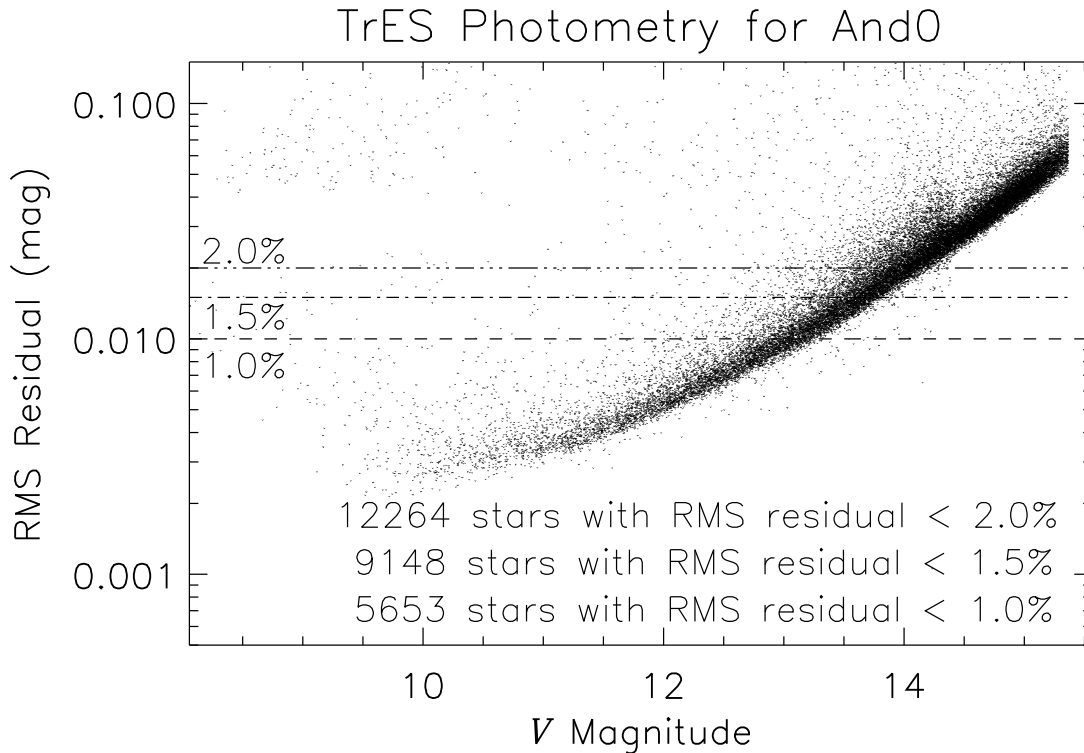


FIG. 3.— The calculated RMS residual of the binned data versus approximate V magnitude for the stars in our TrES And0 data set. The number of stars with RMS below 1%, 1.5%, and 2% are shown. We observed 9,148 stars with the precision required to detect a 1.0% transit lasting 3 hours, assuming we observe at least half the transit from three distinct transit events.

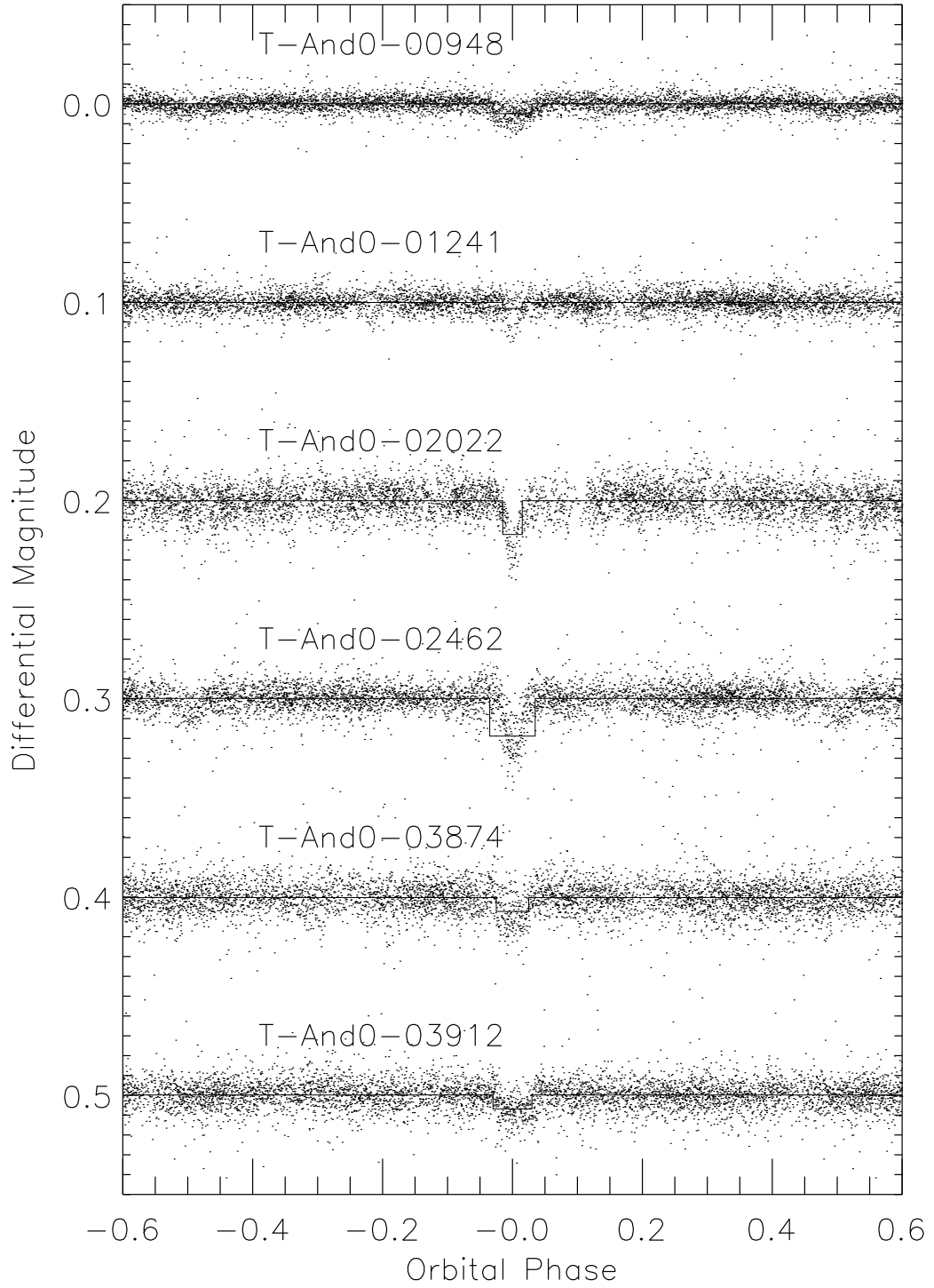


FIG. 4.— The light curves of the six TrES candidates from the combined TrES observations of And0. Again, the best-fit box light curve is plotted over the phased light curve. The TrES light curve of T-And0-00948 confirmed the presence of a secondary eclipse. In the case of T-And0-01241, the TrES light curve is shown phased according to the period derived from the Sleuth data. The transit event is not present in the data from the other telescopes gathered at the same orbital phase.

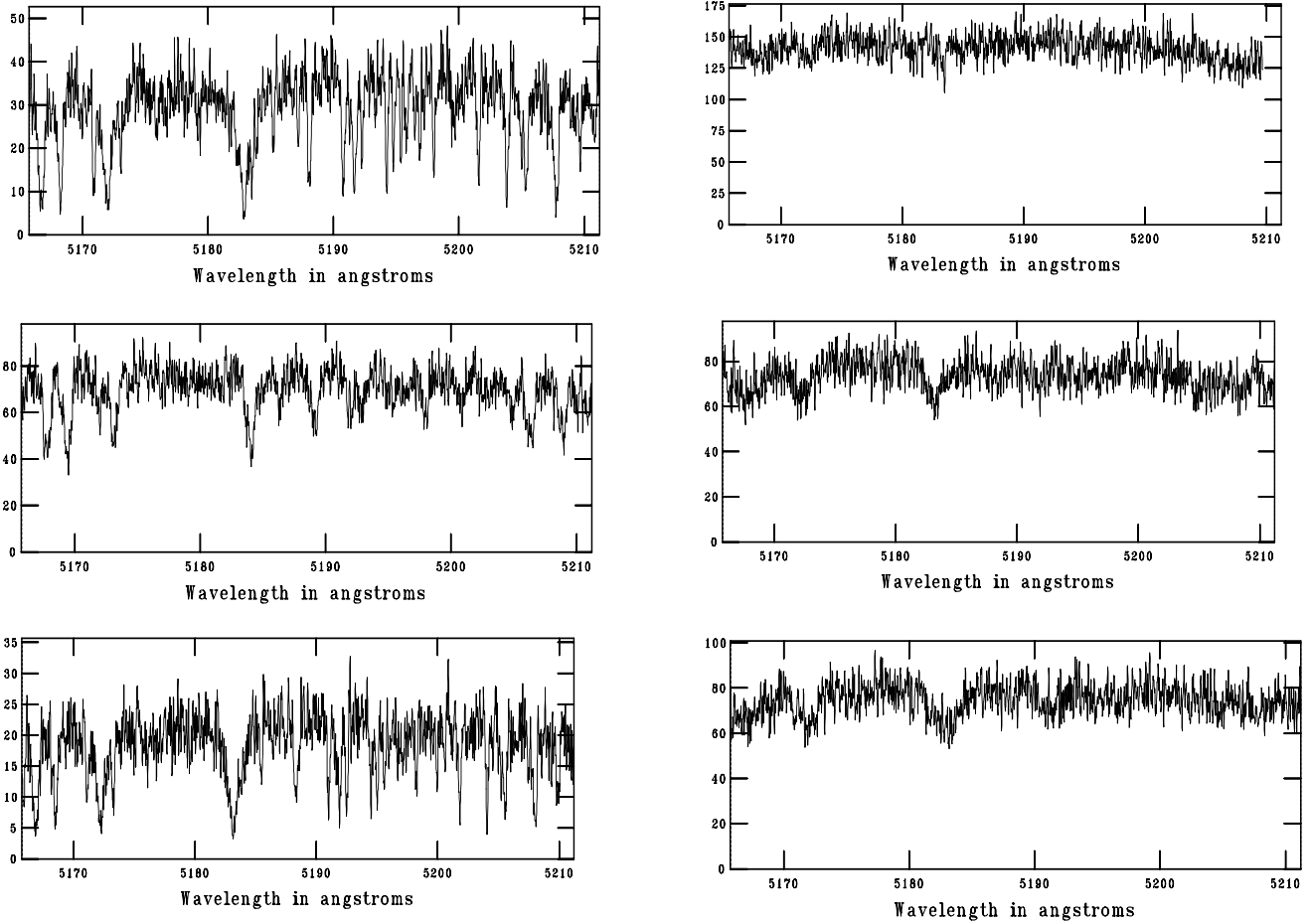


FIG. 5.— Sample spectra of the And0 TrES candidates obtained with the CfA Digital Speedometers on the FLWO 1.5-m telescope: T-And0-00948 (*upper-left*) has the low surface gravity of a giant star; T-And0-01241 (*upper-right*) has the featureless spectrum of an A-type star; T-And0-02022 (*center-left*) is an evolved F dwarf; T-And0-02462 (*center-right*) and T-And0-03912 (*lower-right*) display broadened lines due to the rapid rotation of these stars; T-And0-03874 (*lower-left*) is an early K-type dwarf.

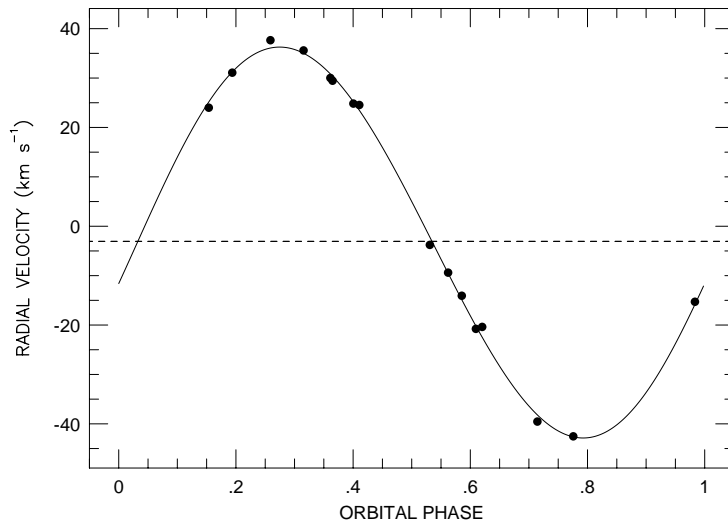


FIG. 6.— The radial velocity orbit of T-And0-02022 as determined from our Digital Speedometer spectra. This system was quickly rejected as a candidate transiting planet after the large radial velocity variation was determined from initial spectroscopic observations. Additional epochs produced a precise orbit, with an eccentricity of $e \sim 0.03$. An initial mass estimate of $0.5 M_{\odot}$ was derived for the companion. Future photometry will lead to more precise mass determination for both component stars (see text for a discussion).

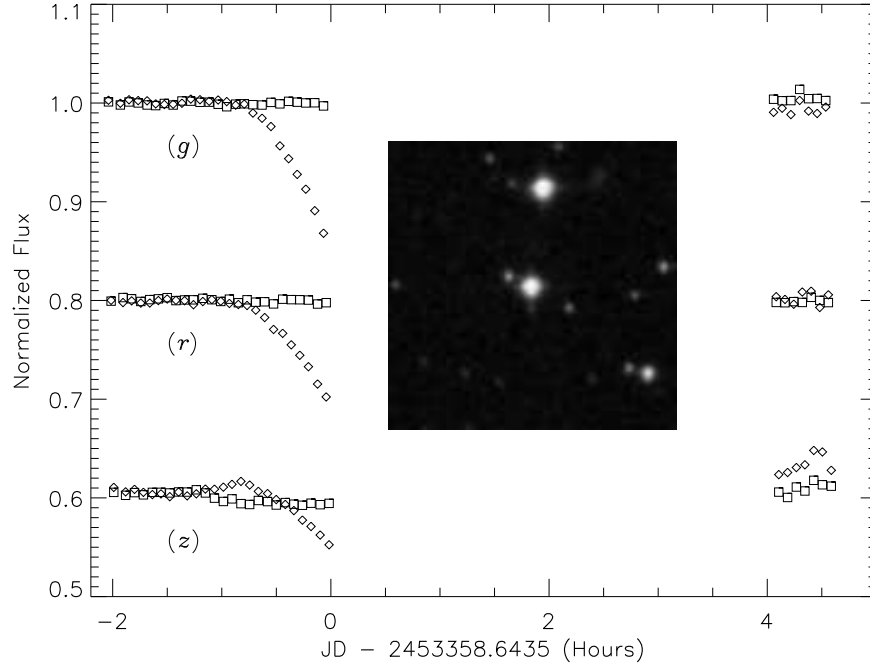


FIG. 7.— Follow-up g , r and z band photometry with the FLWO 1.2-m telescope of T-And0-03874 (*squares*) and a neighboring star (*diamonds*), designated T-And0-02943, that lies $45''$ away. (The inset $2' \times 2'$ Digitized Sky Survey image shows T-And0-03874 at the center and T-And0-02943 to the north.) The flux from each star has been normalized using the out-of-eclipse data, and an offset applied for the purpose of plotting. Inclement weather prevented complete coverage of the predicted eclipse event. Nevertheless, it is evident that T-And0-02943 displays a deep ($> 14\%$) eclipse, whereas the flux from T-And0-03874 is constant. The observed apparent transits of T-And0-03874 were the result of the blending of the light from these two systems. With a FWHM for T-And0-02943 of ~ 2.5 pixels ($\sim 25''$), some of the light from this star was within the photometric aperture radius (3 pixels; $\sim 30''$) of T-And0-03874.

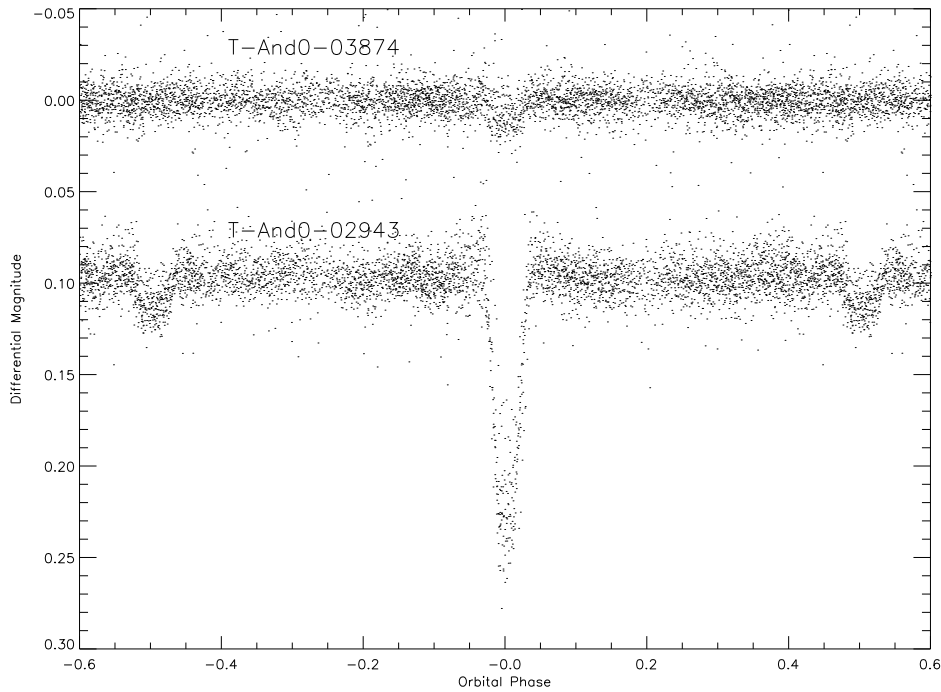


FIG. 8.— TrES photometry of T-And0-03874 and the neighboring eclipsing binary T-And0-02943, phased to the best-fit period (2.6540d) for T-And0-03874 derived by the box-fitting algorithm. Both stars show eclipses with the same orbital period and epoch. The $\sim 1\%$ transit-like event detected in the light curve of T-And0-03874 was the result of the blending of light from this star and from T-And0-02943, which lies $45''$ away, comparable to the $30''$ radius of the TrES PSF.